H. Harbrecht and M. D. Peters

2 Solution of free boundary problems in the presence of geometric uncertainties

Abstract: This chapter is concerned with solving Bernoulli's exterior free boundary problem in the case of an interior boundary which is random. We model this random free boundary problem such that the expectation and the variance of the sought domain can be defined. In order to numerically approximate the expectation and the variance, we propose a sampling method like the (quasi-) Monte Carlo quadrature. The free boundary is determined for each sample by the trial method which is a fixed-point-like iteration. Extensive numerical results are given in order to illustrate the model.

Keywords: Bernoulli's exterior free boundary problem, random boundary

2.1 Introduction

Let $T \subset \mathbb{R}^n$ denote a bounded domain with boundary $\partial T = \Gamma$. Inside the domain T, we assume the existence of a simply connected subdomain $S \subset T$ with boundary $\partial S = \Sigma$. The resulting annular domain $T \setminus \overline{S}$ is denoted by D. The topological situation is visualized in Figure 1.

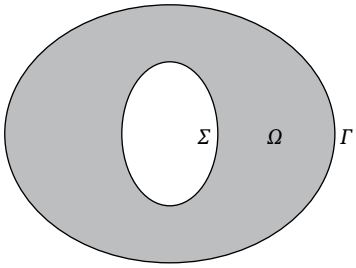

Fig. 1: The domain D and its boundaries Γ and Σ.

We consider the following overdetermined boundary value problem in the annular domain D:

$$\begin{aligned} \Delta u &= 0 && \text{in } D\,, \\ \|\nabla u\| &= f && \text{on } \Gamma\,, \\ u &= 0 && \text{on } \Gamma\,, \\ u &= 1 && \text{on } \Sigma\,, \end{aligned} \tag{1.1}$$

H. Harbrecht, Helmut Harbrecht, Universität Basel, Departement Mathematik und Informatik, Spiegelgasse 1, 4051 Basel, Schweiz, helmut.harbrecht@unibas.ch
M. D. Peters, Michael D. Peters, Universität Basel, Departement Mathematik und Informatik, Spiegelgasse 1, 4051 Basel, Schweiz, michael.peters@unibas.ch

where $f > 0$ is a given constant. We like to stress that the non-negativity of the Dirichlet data implies that u is positive in D. Hence, there holds the identity

$$\|\nabla u\| \equiv -\frac{\partial u}{\partial \mathbf{n}} \quad \text{on } \Gamma \tag{1.2}$$

since u admits homogeneous Dirichlet data on Γ.

We arrive at Bernoulli's exterior free boundary problem if the boundary Γ is unknown. In other words, we seek a domain D with a fixed boundary Σ and unknown boundary Γ such that the overdetermined boundary value problem (1.1) is solvable. This problem has many applications in engineering sciences such as fluid mechanics, see [10], or electromagnetics, see [6, 7] and references therein. In the present form, it models, for example, the growth of anodes in electrochemical processes. For the existence and uniqueness of solutions, we refer the reader to, e.g., [3, 4, 17]; see also [9] for the related interior free boundary problem. Results concerning the geometric form of the solutions can be found in [1] and references therein.

In this chapter, we try to model and solve the free boundary problem (1.1) in the case that the interior boundary is uncertain, i.e., if $\Sigma = \Sigma(\omega)$ with an additional parameter $\omega \in \Omega$. This model is of practical interest in order to treat, for example, tolerances in fabrication processes or if the interior boundary is only known by measurements which typically contain errors. We are thus looking for a tuple $(D(\omega), u(\omega))$ such that it holds

$$\begin{aligned} \Delta u(\omega) &= 0 && \text{in } D(\omega)\,, \\ \|\nabla u(\omega)\| &= f && \text{on } \Gamma(\omega)\,, \\ u(\omega) &= 0 && \text{on } \Gamma(\omega)\,, \\ u(\omega) &= 1 && \text{on } \Sigma(\omega)\,. \end{aligned} \tag{1.3}$$

The questions to be answered in the following are:

- How to model the random domain $D(\omega)$? What is the associated expectation and the variance?
- Do the expectation and the variance exist and are they finite?
- What is the expectation and the variance of the potential $u(\omega)$ if the domain $D(\omega)$ is uncertain?
- How to compute the solution to the random free boundary problem numerically?

For the sake of simplicity, we restrict our consideration to the two-dimensional situation. Nevertheless, the extension to higher dimensions is straightforward and is left to the reader.

The rest of this chapter is organized as follows. Section 2.2 is dedicated to answering the first two questions. We start by defining appropriate function spaces to define the stochastic model. Afterward, we define the random inner boundary and the resulting random outer boundary. Especially, we provide a theorem which guarantees the well posedness of the random free boundary problem under consideration. Moreover,

we introduce here the expectation and the variance of the domain's boundaries. Finally, we give an analytic example which shows that the solution of the free boundary problem depends nonlinearly on the stochastic parameter. In Section 2.3, we answer the latter two questions. We propose the use of boundary integral equations for the solution of the underlying boundary value problem. This significantly decreases the effort for the numerical solution. In particular, we can describe the related potential of the free boundary problem in terms of Green's representation formula. This also allows us to define its expectation and its variance. For the numerical approximation of the free boundary, we apply a trial method in combination with a Nyström discretization of the boundary integral equations. Section 2.4 is then devoted to the numerical examples. We will present here four different examples in order to illustrate different aspects of the proposed approach. We especially show that there is a clear difference between the expected free boundary and the free boundary which belongs to the expected interior boundary. As an important result, it follows thus that one cannot ignore random influences in numerical simulations. Finally, in Section 2.5, we state some concluding remarks.

2.2 Modelling uncertain domains

2.2.1 Notation

In the sequel, let $(\Omega, \mathcal{F}, \mathbb{P})$ denote a complete and separable probability space with σ-algebra $\mathcal{F}$ and probability measure $\mathbb{P}$. Here, complete means that $\mathcal{F}$ contains all $\mathbb{P}$-null sets. In the sequel, for a given Banach space X, the Bochner space $L^p_{\mathbb{P}}(\Omega; X)$, $1 \le p \le \infty$, consists of all equivalence classes of strongly measurable functions $v\colon \Omega \to X$ whose norm

$$\|v\|_{L^p_{\mathbb{P}}(\Omega;X)} := \begin{cases} \left(\int_\Omega \|v(\cdot,\omega)\|_X^p \, \mathrm{d}\mathbb{P}(\omega) \right)^{1/p}, & p < \infty \\ \operatorname*{ess\,sup}_{\omega\in\Omega} \|v(\cdot,\omega)\|_X, & p = \infty \end{cases}$$

is finite. If $p = 2$ and X is a separable Hilbert space, then the Bochner space is isomorphic to the tensor product space $L^2_{\mathbb{P}}(\Omega) \otimes X$. Note that, for notational convenience, we will always write $v(\phi, \omega)$ instead of $(v(\omega))(\phi)$ if $v \in L^p_{\mathbb{P}}(\Omega; X)$. For more details on Bochner spaces, we refer the reader to [14].

2.2.2 Random interior boundary

Throughout the chapter, the domain $D(\omega)$ will be identified by its boundaries $\Sigma(\omega)$ and $\Gamma(\omega)$. Indeed, we assume that $\Sigma(\omega)$ is $\mathbb{P}$-almost surely starlike. This enables us to

parameterize this random boundary in accordance with

$$\Sigma(\omega) = \{\mathbf{x} = \boldsymbol{\sigma}(\phi, \omega) \in \mathbb{R}^2 : \boldsymbol{\sigma}(\phi, \omega) = q(\phi, \omega)\mathbf{e}_r(\phi), \phi \in I\} .$$

Here, $\mathbf{e}_r(\phi) := [\cos(\phi), \sin(\phi)]^\intercal$ is the radial direction and $I := [0, 2\pi]$ is the parameter interval. The radial function $q(\phi, \omega) \geq \underline{c} > 0$ has to be in the Bochner space $L^2(\Omega; C^2_{\text{per}}(I))$, where $C^2_{\text{per}}(I)$ denotes the Banach space of periodic, twice continuously differentiable functions, i.e.,

$$C^2_{\text{per}}(I) := \{f \in C(I) : f^{(i)}(0) = f^{(i)}(2\pi), i = 0, 1, 2\} ,$$

equipped with the norm

$$\|f\|_{C^2_{\text{per}}(I)} := \sum_{i=0}^{2} \max_{x \in I} |f^{(i)}(x)| .$$

For our purposes, we assume that $q(\phi, \omega)$ is described by its expectation

$$\mathbb{E}[q](\phi) = \int_\Omega q(\phi, \omega) \, \mathrm{d}\mathbb{P}(\omega)$$

and its covariance

$$\mathrm{Cov}[q](\phi, \phi') = \mathbb{E}[q(\phi, \omega)q(\phi', \omega)] = \int_\Omega q(\phi, \omega)q(\phi', \omega) \, \mathrm{d}\mathbb{P}(\omega) .$$

Then, $q(\phi, \omega)$ can be represented by the so-called *Karhunen–Loève expansion*, cf. [16],

$$q(\phi, \omega) = \mathbb{E}[q](\phi) + \sum_{k=1}^{N} q_k(\phi) Y_k(\omega) .$$

Herein, the functions $\{q_k(\phi)\}_k$ are scaled versions of the eigenfunctions of the Hilbert–Schmidt operator associated with $\mathrm{Cov}[q](\phi, \phi')$. Common approaches to numerically recover the Karhunen–Loève expansion from these quantities are, e.g., given in [13] and the references therein. By construction, the random variables $\{Y_k(\omega)\}_k$ in the Karhunen–Loève expansion are uncorrelated. For our modelling, we shall also require that they are independent, which is a common assumption. Moreover, we suppose that they are identically distributed with $\mathrm{img}\, Y_k(\omega) = [-1, 1]$. Note that it holds

$$\mathbb{V}[q](\phi) = \int_\Omega \{q(\phi, \omega) - \mathbb{E}[q](\phi)\}^2 \, \mathrm{d}\mathbb{P}(\omega) = \sum_{k=1}^{N} (q_k(\phi))^2 .$$

2.2.3 Random exterior boundary

If the interior boundary $\Sigma(\omega)$ is starlike, then also the exterior boundary $\Gamma(\omega)$ is starlike. In particular, it also follows that the free boundary $\Gamma(\omega)$ is C^∞-smooth, see [2]

for details. Hence, the exterior boundary can likewise be represented via its parameterization:

$$\Gamma(\omega) = \{\mathbf{x} = \boldsymbol{\gamma}(\phi, \omega) \in \mathbb{R}^2 : \boldsymbol{\gamma}(\phi, \omega) = r(\phi, \omega)\mathbf{e}_r(\phi), \phi \in I\} . \tag{2.1}$$

The following theorem guarantees us the well posedness of the problem under consideration, cf. [4, 17]. It shows that it holds $r(\phi, \omega) \in L^\infty_{\mathbb{P}}(\Omega, C^2_{\mathrm{per}}(I))$ if $q(\phi, \omega)$ is almost surely bounded and thus that $\boldsymbol{\gamma}(\phi, \omega)$ is well defined.

Theorem 2.1. *Assume that $q(\phi, \omega)$ is uniformly bounded almost surely, i.e.,*

$$q(\phi, \omega) \leq \underline{R} \quad \text{for all } \phi \in I \text{ and } \mathbb{P}\text{-almost every } \omega \in \Omega . \tag{2.2}$$

Then, there exists a unique solution $(D(\omega), u(\omega))$ to (1.3) for almost every $\omega \in \Omega$. Especially, with some constant $\overline{R} > \underline{R}$, the radial function $r(\phi, \omega)$ of the associated free boundary (2.1) satisfies

$$q(\phi, \omega) < r(\phi, \omega) \leq \overline{R} \quad \text{for all } \phi \in I \text{ and } \mathbb{P}\text{-almost every } \omega \in \Omega .$$

Proof. In view of (2.2), it follows that

$$\Sigma(\omega) \subset B_{\underline{R}}(\mathbf{0}) := \{\mathbf{x} \in \mathbb{R}^2 : \|\mathbf{x}\| < \underline{R}\}$$

for almost every $\omega \in \Omega$. Hence, for fixed $\omega \in \Omega$, [17, Theorem 1] guarantees the unique solvability of (1.3). In particular, there exists a constant $\overline{R} > \underline{R}$ such that $\Gamma(\omega) \subset B_{\overline{R}}(\mathbf{0})$ whenever $\Sigma(\omega) \subset B_{\underline{R}}(\mathbf{0})$. Therefore, the claim follows since $q(\phi, \omega)$ is supposed to be uniformly bounded in $\omega \in \Omega$. □

2.2.4 Expectation and variance of the domain

Having the parameterizations $\boldsymbol{\sigma}(\omega)$ and $\boldsymbol{\gamma}(\omega)$ at hand, we can obtain the expectation and the variance of the domain $D(\omega)$.

Theorem 2.2. *The expectation of the domain $D(\omega)$ is given via the expectations of its boundaries' parameterizations in accordance with*

$$\mathbb{E}[\partial D(\omega)] = \mathbb{E}[\Sigma(\omega)] \cup \mathbb{E}[\Gamma(\omega)] ,$$

where

$$\mathbb{E}[\Sigma(\omega)] = \{\mathbf{x} \in \mathbb{R}^2 : \mathbf{x} = \mathbb{E}[q(\phi, \omega)]\mathbf{e}_r(\phi), \phi \in I\} ,$$
$$\mathbb{E}[\Gamma(\omega)] = \{\mathbf{x} \in \mathbb{R}^2 : \mathbf{x} = \mathbb{E}[r(\phi, \omega)]\mathbf{e}_r(\phi), \phi \in I\} .$$

Proof. For the proof, we introduce the global parameterization $\boldsymbol{\delta} : [0, 4\pi) \to \partial D(\omega)$ given by

$$\boldsymbol{\delta}(\phi, \omega) = \begin{cases} \boldsymbol{\sigma}(\phi, \omega), & \phi \in [0, 2\pi) , \\ \boldsymbol{\gamma}(\phi - 2\pi, \omega), & \phi \in [2\pi, 4\pi) . \end{cases} \tag{2.3}$$

Then, it holds per definition that

$$\mathbb{E}[\partial D(\omega)] = \{\mathbf{x} \in \mathbb{R}^2 : \mathbf{x} = \mathbb{E}[\boldsymbol{\delta}(\phi, \omega)], \phi \in [0, 4\pi)\} .$$

Therefore, the expected boundary $\mathbb{E}[\partial D(\omega)]$ consists of all points $\mathbf{x} \in \mathbb{R}^2$ with

$$\mathbf{x} = \begin{cases} \mathbb{E}[\boldsymbol{\sigma}(\phi, \omega)], & \phi \in [0, 2\pi) , \\ \mathbb{E}[\boldsymbol{\gamma}(\phi - 2\pi, \omega)], & \phi \in [2\pi, 4\pi) . \end{cases}$$

This is equivalent to

$$\mathbf{x} = \begin{cases} \mathbb{E}[q(\phi, \omega)]\mathbf{e}_r(\phi), & \phi \in [0, 2\pi) , \\ \mathbb{E}[r(\phi - 2\pi, \omega)]\mathbf{e}_r(\phi - 2\pi), & \phi \in [2\pi, 4\pi) , \end{cases}$$

which immediately implies the assertion. □

The variance of the domain $D(\omega)$ is obtained in a similar way as the expectation. In particular, it suffices to take only the radial part of the variance into account due to the star shapedness.

Theorem 2.3. *The variance of the domain $D(\omega)$ in the radial direction is given via the variances of its boundaries parameterizations in accordance with*

$$\mathbb{V}[\partial D(\omega)] = \mathbb{V}[\Sigma(\omega)] \cup \mathbb{V}[\Gamma(\omega)]$$

where

$$\mathbb{V}[\Sigma(\omega)] = \{\mathbf{x} \in \mathbb{R}^2 : \mathbf{x} = \mathbb{V}[q(\phi, \omega)]\mathbf{e}_r(\phi), \phi \in I\} ,$$
$$\mathbb{V}[\Gamma(\omega)] = \{\mathbf{x} \in \mathbb{R}^2 : \mathbf{x} = \mathbb{V}[r(\phi, \omega)]\mathbf{e}_r(\phi), \phi \in I\} .$$

Proof. We shall again employ the global parameterization $\boldsymbol{\delta}(\phi, \omega)$ from (2.3). For the sake of notational convenience, we denote its centered version by

$$\boldsymbol{\delta}_0(\phi, \omega) := \boldsymbol{\delta}(\phi, \omega) - \mathbb{E}[\boldsymbol{\delta}(\phi, \omega)] ,$$

and likewise for $\boldsymbol{\sigma}(\phi, \omega)$ and $\boldsymbol{\gamma}(\phi, \omega)$.

The variance of $D(\omega)$ can be determined as the trace of the covariance

$$\mathrm{Cov}[\partial D(\omega)] = \{\mathbf{X} \in \mathbb{R}^{2\times 2} : \mathbf{X} = \mathbb{E}[\boldsymbol{\delta}_0(\phi, \omega)\boldsymbol{\delta}_0(\phi', \omega)^\intercal], \phi \in [0, 4\pi)\} .$$

From this representation, one concludes that $\mathrm{Cov}[\partial D(\omega)]$ consists of all (2×2) matrices $\mathbf{X}$ with

$$\mathbf{X} = \begin{cases} \mathbb{E}[\boldsymbol{\sigma}_0(\phi, \omega)\boldsymbol{\sigma}_0(\phi', \omega)^\intercal], & \phi, \phi' \in [0, 2\pi) , \\ \mathbb{E}[\boldsymbol{\sigma}_0(\phi, \omega)\boldsymbol{\gamma}_0(\phi' - 2\pi, \omega)^\intercal], & \phi \in [0, 2\pi), \phi' \in [2\pi, 4\pi) , \\ \mathbb{E}[\boldsymbol{\gamma}_0(\phi - 2\pi, \omega)\boldsymbol{\sigma}_0(\phi', \omega)^\intercal], & \phi \in [2\pi, 4\pi), \phi' \in [0, 2\pi) , \\ \mathbb{E}[\boldsymbol{\gamma}_0(\phi - 2\pi, \omega)\boldsymbol{\gamma}_0(\phi' - 2\pi, \omega)^\intercal], & \phi, \phi' \in [2\pi, 4\pi) . \end{cases}$$

The situation $\phi = \phi'$ can only appear in the first or last case. These can be reformulated with $\phi, \phi' \in [0, 2\pi)$ as

$$\begin{aligned}\mathrm{Cov}[\boldsymbol{\sigma}, \boldsymbol{\sigma}](\phi, \phi') &= \mathbb{E}\big[\boldsymbol{\sigma}_0(\phi, \omega)\boldsymbol{\sigma}_0(\phi', \omega)^\intercal\big] \\ &= \mathbb{E}\big[\big(q(\phi, \omega) - \mathbb{E}[q](\phi)\big)\big(q(\phi', \omega) - \mathbb{E}[q](\phi)\big)\big]\mathbf{e}_r(\phi)\mathbf{e}_r(\phi')^\intercal\end{aligned}$$

and likewise as

$$\begin{aligned}\mathrm{Cov}[\boldsymbol{\gamma}, \boldsymbol{\gamma}](\phi, \phi') &= \mathbb{E}\big[\boldsymbol{\gamma}_0(\phi, \omega)\boldsymbol{\gamma}_0(\phi', \omega)^\intercal\big] \\ &= \mathbb{E}\big[\big(r(\phi, \omega) - \mathbb{E}[r](\phi)\big)\big(r(\phi', \omega) - \mathbb{E}[r](\phi)\big)\big]\mathbf{e}_r(\phi)\mathbf{e}_r(\phi')^\intercal\,.\end{aligned}$$

By setting $\phi = \phi'$, we arrive at

$$\mathrm{Cov}[\boldsymbol{\sigma}, \boldsymbol{\sigma}](\phi, \phi) = \mathbb{V}[q](\phi)\mathbf{e}_r(\phi)\mathbf{e}_r(\phi)^\intercal \text{ and } \mathrm{Cov}[\boldsymbol{\gamma}, \boldsymbol{\gamma}](\phi, \phi) = \mathbb{V}[q](\phi)\mathbf{e}_r(\phi)\mathbf{e}_r(\phi)^\intercal\,.$$

To get the radial part of the variances, we multiply the last expression by the radial direction $\mathbf{e}_r$ which yields the desired assertion. □

Consequently, in view of having $\mathbb{E}[q(\phi, \omega)]$ and $\mathbb{V}[q(\phi, \omega)]$ at hand, we need just to compute the expectation $\mathbb{E}[r(\phi, \omega)]$ and the variance $\mathbb{V}[r(\phi, \omega)]$ to obtain the expectation and the variance of the random domain $D(\omega)$.

2.2.5 Stochastic quadrature method

For numerical simulation, we aim at approximating $\mathbb{E}[r(\phi, \omega)]$ and $\mathbb{V}[r(\phi, \omega)]$ with the aid of a (quasi-) Monte Carlo quadrature. To that end, we first parameterize the stochastic influences in $q(\phi, \omega)$ by considering the parameter domain $\square := [-1, 1]^N$ and setting

$$q(\phi, \mathbf{y}) = \mathbb{E}[q](\phi) + \sum_{k=1}^{N} q_k(\phi)y_k \quad \text{for } \mathbf{y} = [y_1, \ldots, y_N]^\intercal \in \square\,.$$

Especially, we have $q(\phi, \mathbf{y}) \in L^\infty\big(\square; C^2_{\mathrm{per}}(I)\big)$ if $q(\phi, \omega) \in L^\infty\big(\Omega; C^2_{\mathrm{per}}(I)\big)$. Here, the space $L^\infty\big(\square; C^2_{\mathrm{per}}(I)\big)$ is equipped with the pushforward measure $\mathbb{P}_{\mathbf{Y}}$, where $\mathbf{Y} = [Y_1, \ldots, Y_N]^\intercal$. This measure is of product structure due to the independence of the random variables. If the measure $\mathbb{P}_{\mathbf{Y}}$ is absolutely continuous with respect to the Lebesgue measure, then there exists a density $\rho(\mathbf{y})$, which is also of product structure, such that there holds

$$\mathbb{E}[q](\phi) = \int_\Omega q(\phi, \omega)\,\mathrm{d}\mathbb{P}(\omega) = \int_\square q(\phi, \mathbf{y})\rho(\mathbf{y})\,\mathrm{d}\mathbf{y}\,.$$

In complete analogy, we have for the variance

$$\mathbb{V}[q](\phi) = \int_\Omega \big(q(\phi, \omega)\big)^2\,\mathrm{d}\mathbb{P}(\omega) - \big(\mathbb{E}[q](\phi)\big)^2 = \int_\square \big(q(\phi, \mathbf{y})\big)^2\rho(\mathbf{y})\,\mathrm{d}\mathbf{y} - \big(\mathbb{E}[q](\phi)\big)^2\,.$$

Now, if

$$F\colon L^\infty(\Omega; C^2_{\mathrm{per}}(I)) \to L^\infty(\Omega; C^2_{\mathrm{per}}(I)), \quad q(\phi, \omega) \mapsto r(\phi, \omega) \tag{2.4}$$

denotes the solution map, the expectation and the variance of $r(\phi, \omega)$ are given according to

$$\mathbb{E}[r](\phi) = \mathbb{E}[F(q)](\phi) \quad \text{and} \quad \mathbb{V}[r](\phi) = \mathbb{V}[F(q)](\phi)\,.$$

In view of this representation, we can apply a (quasi-) Monte Carlo quadrature in order to approximate the desired quantities.

The Monte Carlo quadrature and the quasi-Monte Carlo quadrature approximate the integral of a sufficiently smooth function f over $\square$ by a weighted sum according to

$$\int_{\square} f(\mathbf{y})\,\mathrm{d}\mathbf{y} \approx \frac{1}{M}\sum_{i=1}^{M} f(\mathbf{y}_i)\,.$$

Herein, the sample points $\{\mathbf{y}_1, \ldots, \mathbf{y}_M\}$ are either chosen randomly with respect to the uniform distribution, which results in the Monte Carlo quadrature, or according to a deterministic low-discrepancy sequence, which results in the quasi-Monte Carlo quadrature. The Monte Carlo quadrature can be shown to converge, in the mean square sense, with a dimension-independent rate of $M^{-1/2}$. The quasi-Monte Carlo quadrature based, for example, on Halton points, cf. [11], converges instead with the rate $M^{\delta-1}$ for arbitrary $\delta > 0$. Although, for the quasi-Monte Carlo quadrature, the integrand has to provide bounded first-order mixed derivatives. For more details on this topic, see [5] and the references therein.

In our particular problem under consideration, the expectation $\mathbb{E}[r](\phi)$ and the variance $\mathbb{V}[r](\phi)$ are finally computed in accordance with

$$\mathbb{E}[r](\phi) = \mathbb{E}[F(q)](\phi) \approx \frac{1}{M}\sum_{i=1}^{M} F\big(q(\phi, \mathbf{y}_i)\big)\rho(\mathbf{y}_i)$$

and

$$\mathbb{V}[r](\phi) = \mathbb{V}[F(q)](\phi) \approx \frac{1}{M}\sum_{i=1}^{M} \Big(F\big(q(\phi, \mathbf{y}_i)\big)\Big)^2\rho(\mathbf{y}_i) - \left(\frac{1}{M}\sum_{i=1}^{M} F\big(q(\phi, \mathbf{y}_i)\big)\rho(\mathbf{y}_i)\right)^2.$$

2.2.6 Analytical example

The calculations can be performed analytically if the interior boundary $\Sigma(\omega)$ is a circle around the origin with radius $q(\omega)$. Then, due to symmetry, also the free boundary $\Gamma(\omega)$ will be a circle around the origin with unknown radius $r(\omega)$. We shall thus focus on this particular situation in order to verify that the radius $r(\omega)$ depends nonlinearly on the stochastic input $q(\omega)$. Hence, on the associated expected domain $\mathbb{E}[D(\omega)]$, the overdetermined boundary value problem (1.1) has, in general, no solution.

Using polar coordinates and making the ansatz $|u(\rho, \phi)| = y(\rho)$, the solution with respect to the prescribed Dirichlet boundary condition of (1.1) has to satisfy

$$y'' + \frac{y'}{\rho} = 0, \quad y(q(\omega)) = 1, \quad y(r(\omega)) = 0 .$$

The solution to this boundary value problem is given by

$$y(\rho) = \frac{\log\left(\frac{\rho}{r(\omega)}\right)}{\log\left(\frac{q(\omega)}{r(\omega)}\right)} .$$

The desired Neumann boundary condition at the free boundary $r(\omega)$ yields the equation

$$-y'(r(\omega)) = \frac{1}{r(\omega)\log\left(\frac{r(\omega)}{q(\omega)}\right)} \stackrel{!}{=} f ,$$

which can be solved by means of Lambert's W-function:

$$r(\omega) = \frac{1}{fW\left(\frac{1}{fq(\omega)}\right)} . \tag{2.5}$$

Thus, the free boundary $r(\omega)$ depends nonlinearly on $q(\omega)$ since it generally holds

$$\mathbb{E}[r(\omega)] = \mathbb{E}\left[\frac{1}{fW\left(\frac{1}{fq(\omega)}\right)}\right] \neq \frac{1}{fW\left(\frac{1}{f\mathbb{E}[q]}\right)} . \tag{2.6}$$

Notice that the right-hand side would be the (unique) solution of the free boundary problem in the case of the interior circle of radius $\mathbb{E}[q(\omega)]$. Thus, indeed the overdetermined boundary value problem (1.1) will, in general, not be fulfilled on the expected domain $\mathbb{E}[D(\omega)]$.

2.3 Computing free boundaries

2.3.1 Trial method

For computing the expected domain $\mathbb{E}[D(\omega)]$ and its variance $\mathbb{V}[D(\omega)]$, we have to be able to determine the free boundary $\Gamma(\omega)$ for each specific realization of the fixed boundary $\Sigma(\omega)$. This will be done by the so-called trial method, which is a fixed point type iterative scheme. For the sake of simplicity in representation, we omit the stochastic variable ω in this section, i.e., we assume that $\omega \in \Omega$ is fixed.

The trial method for the solution of the free boundary problem (1.1) requires an update rule. Suppose that the current boundary in the k-th iteration is Γ_k and let the current state u_k satisfy

$$\begin{aligned} \Delta u_k &= 0 && \text{in } D_k , \\ u_k &= 1 && \text{on } \Sigma , \\ -\frac{\partial u_k}{\partial \mathbf{n}} &= f && \text{on } \Gamma_k . \end{aligned} \tag{3.1}$$

The new boundary Γ_{k+1} is now determined by moving the old boundary into the radial direction, which is expressed by the update rule

$$\boldsymbol{\gamma}_{k+1} = \boldsymbol{\gamma}_k + \delta r_k \mathbf{e}_r \,.$$

The update function $\delta r_k \in C^2_{\mathrm{per}}([0, 2\pi])$ is chosen such that the desired homogeneous Dirichlet boundary condition is approximately satisfied at the new boundary Γ_{k+1}, i.e.,

$$0 \stackrel{!}{=} u_k \circ \boldsymbol{\gamma}_{k+1} \approx u_k \circ \boldsymbol{\gamma}_k + \left(\frac{\partial u_k}{\partial \mathbf{e}_r} \circ \boldsymbol{\gamma}_k \right) \delta r_k \quad \text{on } [0, 2\pi] \,, \tag{3.2}$$

where u_k is assumed to be smoothly extended into the exterior of the domain D_k. We decompose the derivative of u_k in the direction $\mathbf{e}_r$ into its normal and tangential components

$$\frac{\partial u_k}{\partial \mathbf{e}_r} = \frac{\partial u_k}{\partial \mathbf{n}} \langle \mathbf{e}_r, \mathbf{n} \rangle + \frac{\partial u_k}{\partial \mathbf{t}} \langle \mathbf{e}_r, \mathbf{t} \rangle \quad \text{on } \Gamma_k \tag{3.3}$$

to arrive finally at the following iterative scheme (cf. [9, 12, 18]):

(1) Choose an initial guess Γ_0 of the free boundary.

(2a) Solve the boundary value problem with the Neumann boundary condition on the free boundary Γ_k.

(2b) Update the free boundary Γ_k such that the Dirichlet boundary condition is approximately satisfied at the new boundary Γ_{k+1}:

$$\delta r_k = -\frac{u_k}{\frac{\partial u_k}{\partial \mathbf{e}_r}} = -\frac{u_k}{f \langle \mathbf{n}, \mathbf{e}_r \rangle + \frac{\partial u_k}{\partial \mathbf{t}} \langle \mathbf{t}, \mathbf{e}_r \rangle} \,. \tag{3.4}$$

(3) Repeat step 2 until the process becomes stationary up to a specified accuracy.

Notice that the update equation (3.4) is always solvable at least in a neighborhood of the optimum free boundary Γ since there it holds $-\partial u / \partial \mathbf{e}_r = f \langle \mathbf{e}_r, \mathbf{n} \rangle > 0$ due to $\partial u_k / \partial \mathbf{t} = 0$, $f > 0$ and $\langle \mathbf{e}_r, \mathbf{n} \rangle > 0$ for starlike domains.

2.3.2 Discretizing the free boundary

For the numerical computations, we discretize the radial function r_k associated with the boundary Γ_k by a trigonometric polynomial according to

$$r_k(\phi) = \frac{a_0}{2} + \sum_{i=1}^{n-1} \{ a_i \cos(i\phi) + b_i \sin(i\phi) \} + \frac{a_n}{2} \cos(n\phi) \,. \tag{3.5}$$

This obviously ensures that r_k is always an element of $C^2_{\mathrm{per}}(I)$. To determine the update function δr_k, represented likewise by a trigonometric polynomial, we insert the $m \geq 2n$ equidistantly distributed points $\phi_i = 2\pi i / m$ into the update equation (3.4):

$$\delta r_k = -\frac{u_k}{f \langle \mathbf{n}, \mathbf{e}_r \rangle + \frac{\partial u_k}{\partial \mathbf{t}} \langle \mathbf{t}, \mathbf{e}_r \rangle} \quad \text{in all the points } \phi_1, \ldots, \phi_m \,.$$

This is a discrete least-squares problem which can simply be solved by the normal equations. In view of the orthogonality of the Fourier basis, this means just a truncation of the trigonometric polynomial.

2.3.3 Boundary integral equations

Our approach to determine the solution u_k of the state equation (3.1) relies on the reformulation as a boundary integral equation by using Green's fundamental solution

$$G(\mathbf{x}, \mathbf{y}) = -\frac{1}{2\pi} \log \|\mathbf{x} - \mathbf{y}\|_2 \, .$$

Namely, the solution $u_k(\mathbf{x})$ of (3.1) is given in each point $\mathbf{x} \in D$ by Green's representation formula

$$u_k(\mathbf{x}) = \int_{\Gamma_k \cup \Sigma} \left\{ G(\mathbf{x}, \mathbf{y}) \frac{\partial u_k}{\partial \mathbf{n}}(\mathbf{y}) - \frac{\partial G(\mathbf{x}, \mathbf{y})}{\partial \mathbf{n}_\mathbf{y}} u_k(\mathbf{y}) \right\} \mathrm{d}\sigma_\mathbf{y} \, . \tag{3.6}$$

Using the jump properties of the layer potentials, we obtain the direct boundary integral formulation of the problem

$$\frac{1}{2} u_k(\mathbf{x}) = \int_{\Gamma_k \cup \Sigma} G(\mathbf{x}, \mathbf{y}) \frac{\partial u_k}{\partial \mathbf{n}}(\mathbf{y}) \, \mathrm{d}\sigma_\mathbf{y} - \int_{\Gamma_k \cup \Sigma} \frac{\partial G(\mathbf{x}, \mathbf{y})}{\partial \mathbf{n}_\mathbf{y}} u_k(\mathbf{y}) \, \mathrm{d}\sigma_\mathbf{y} \, , \tag{3.7}$$

where $\mathbf{x} \in \Gamma_k \cup \Sigma$. If we label the boundaries by $A, B \in \{\Gamma_k, \Sigma\}$, then (3.7) includes the single-layer operator

$$\mathcal{V} \colon C(A) \to C(B), \quad (\mathcal{V}_{AB}\rho)(\mathbf{x}) = -\frac{1}{2\pi} \int_A \log \|\mathbf{x} - \mathbf{y}\|_2 \, \rho(\mathbf{y}) \, \mathrm{d}\sigma_\mathbf{y} \tag{3.8}$$

and the double-layer operator

$$\mathcal{K} \colon C(A) \to C(B), \quad (\mathcal{K}_{AB}\rho)(\mathbf{x}) = \frac{1}{2\pi} \int_A \frac{\langle \mathbf{x} - \mathbf{y}, \mathbf{n}_\mathbf{y} \rangle}{\|\mathbf{x} - \mathbf{y}\|_2^2} \rho(\mathbf{y}) \, \mathrm{d}\sigma_\mathbf{y} \tag{3.9}$$

with the densities $\rho \in C(A)$ being the Cauchy data of u on A. Equation (3.7) in combination with (3.8) and (3.9) indicates the Neumann-to-Dirichlet map, which for problem (3.1) induces the following system of integral equations:

$$\begin{bmatrix} \frac{1}{2} I + \mathcal{K}_{\Gamma\Gamma} & -\mathcal{V}_{\Sigma\Gamma} \\ \mathcal{K}_{\Gamma\Sigma} & -\mathcal{V}_{\Sigma\Sigma} \end{bmatrix} \begin{bmatrix} u_k|_\Gamma \\ \frac{\partial u_k}{\partial \mathbf{n}}|_\Sigma \end{bmatrix} = \begin{bmatrix} \mathcal{V}_{\Gamma\Gamma} & -\mathcal{K}_{\Sigma\Gamma} \\ \mathcal{V}_{\Gamma\Sigma} & -(\frac{1}{2} I + \mathcal{K}_{\Sigma\Sigma}) \end{bmatrix} \begin{bmatrix} -f \\ 1 \end{bmatrix} \, . \tag{3.10}$$

The boundary integral operator on the left-hand side of this coupled system of the boundary integral equation is continuous and satisfies a Gårding inequality with respect to the product Sobolev space $L^2(\Gamma) \times H^{-1/2}(\Sigma)$ provided that $\mathrm{diam}(\Omega) < 1$.

Since its injectivity follows from potential theory, this system of integral equations is uniquely solvable according to the Riesz–Schauder theory.

The next step to the solution of the boundary value problem is the numerical approximation of the integral operators included in (3.10) which first requires the parameterization of the integral equations. To that end, we insert the parameterizations $\boldsymbol{\sigma}$ and $\boldsymbol{\gamma}_k$ of the boundaries Σ and Γ_k, respectively. For the approximation of the unknown Cauchy data, we use the collocation method based on trigonometric polynomials. Applying the trapezoidal rule for the numerical quadrature and the regularization technique along the lines of [15] to deal with the singular integrals, we arrive at an exponentially convergent Nyström method provided that the data and the boundaries and thus the solution are arbitrarily smooth.

2.3.4 Expectation and variance of the potential

We shall comment on the expectation and the variance of the potential. To that end, we consider a specific sample $\omega \in \Omega$ and assume that the associated free boundary $\Gamma(\omega)$ is known. Then, with the aid of the parameterizations

$$\boldsymbol{\sigma}(\omega)\colon [0, 2\pi] \to \Sigma(\omega) \quad \text{and} \quad \boldsymbol{\gamma}(\omega)\colon [0, 2\pi] \to \Gamma(\omega)\,,$$

we arrive, in view of (3.6), for $\mathbf{x} \in D(\omega)$ at the potential representation

$$u(\mathbf{x}, \omega) = \sum_{A \in \{\Sigma(\omega), \Gamma(\omega)\}} \int_0^{2\pi} \{k_A^{\mathcal{V}}(\mathbf{x}, \phi, \omega)\rho_A^{\mathcal{V}}(\phi, \omega) - k_A^{\mathcal{K}}(\mathbf{x}, \phi, \omega)\rho_A^{\mathcal{K}}(\phi, \omega)\}\, \mathrm{d}\phi\,, \quad (3.11)$$

where

$$k_{\Sigma(\omega)}^{\mathcal{V}}(\mathbf{x}, \phi, \omega) = G(\mathbf{x}, \boldsymbol{\sigma}(\phi, \omega))\|\boldsymbol{\sigma}'(\phi, \omega)\|_2\,,$$
$$k_{\Gamma(\omega)}^{\mathcal{V}}(\mathbf{x}, \phi, \omega) = G(\mathbf{x}, \boldsymbol{\gamma}(\phi, \omega))\|\boldsymbol{\gamma}'(\phi, \omega)\|_2\,,$$

and

$$k_{\Sigma(\omega)}^{\mathcal{K}}(\mathbf{x}, \phi, \omega) = \frac{\partial G(\mathbf{x}, \boldsymbol{\sigma}(\phi, \omega))}{\partial \mathbf{n}_{\mathbf{y}}}\|\boldsymbol{\sigma}'(\phi, \omega)\|_2\,,$$
$$k_{\Gamma(\omega)}^{\mathcal{K}}(\mathbf{x}, \phi, \omega) = \frac{\partial G(\mathbf{x}, \boldsymbol{\gamma}(\phi, \omega))}{\partial \mathbf{n}_{\mathbf{y}}}\|\boldsymbol{\gamma}'(\phi, \omega)\|_2\,.$$

Moreover, the related densities are given according to

$$\rho_{\Sigma(\omega)}^{\mathcal{V}}(\phi, \omega) = \frac{\partial u}{\partial \mathbf{n}}(\boldsymbol{\sigma}(\phi, \omega)), \quad \rho_{\Gamma(\omega)}^{\mathcal{V}}(\phi, \omega) = \frac{\partial u}{\partial \mathbf{n}}(\boldsymbol{\gamma}(\phi, \omega))\,,$$
$$\rho_{\Sigma(\omega)}^{\mathcal{K}}(\phi, \omega) = u(\boldsymbol{\sigma}(\phi, \omega)), \qquad \rho_{\Gamma(\omega)}^{\mathcal{K}}(\phi, \omega) = u(\boldsymbol{\gamma}(\phi, \omega))\,.$$

These densities coincide with the Cauchy data of the potential $u(\omega)$ on the boundary $\partial D(\omega)$.

In view of the representation (3.11), we observe that the expectation $\mathbb{E}[u](\mathbf{x})$ and the variance $\mathbb{V}[u](\mathbf{x})$ of the potential depend nonlinearly on the random parameter $\omega \in \Omega$. This is due to the fact that, in contrast to, e.g., [8], not only the density depends on ω but also the kernel function because of the parameterization. Nevertheless, if desired, these quantities can easily be approximated by sampling the expression (3.11) and its squared form for different realizations of the random parameter $\omega \in \Omega$ by a (quasi-) Monte Carlo method as already discussed in Section 2.2.4 for $r(\phi, \omega)$.

2.4 Numerical results

In this section, we provide several numerical examples in order to illustrate our approach. For the numerical solution of the free boundary problem for each instance of the random parameter $\omega \in \Omega$, we apply the trial method proposed in the preceding section. The iteration is stopped if the ℓ^∞-norm of the update becomes smaller than 10^{-7}. For the discretization of the free boundary, we employ a trigonometric polynomial of order 32, i.e., $n = 16$ in (3.5). For the collocation method, we use $m = 200$ collocation points.

2.4.1 First example

Our first example refers to the analytical example presented in Section 2.2.6. In particular, we want to illustrate that the expectation of the free boundary $\Gamma(\omega)$ differs from the free boundary obtained for given $\mathbb{E}[\Sigma]$. To that end, we consider the following situation: In (1.3), we set $u(\omega) = 1$ on $\Sigma(\omega)$ and $\|\nabla u(\omega)\|_2 = 10$ on $\Gamma(\omega)$. Moreover, we set $q(\phi, \omega) = 0.2 + 0.195X(\omega)$, where X is distributed with respect to the counting measure $\mu(x) = 0.5 \cdot \delta_{-1}(x) + 0.5 \cdot \delta_1(x)$. Therefore, we can exactly determine the expectation and the variance of the free boundary by just two realizations of $q(\phi, \omega)$.

On the left-hand side of Figure 2, a visualization of the random domain's statistics is found. The green line belongs to the expectation of the inner boundary $\mathbb{E}[\Sigma]$. The expectation of the free boundary $\mathbb{E}[\Gamma]$ is indicated by the blue line. The gray shaded area refers to the standard deviation of Γ with respect to the expectation, i.e., the area which is bounded by $\mathbb{E}[\Gamma] \pm \sqrt{\mathbb{V}[\Gamma]}$. Moreover, we have depicted the solution to the free boundary problem for the fixed inner boundary $\mathbb{E}[\Sigma]$, i.e., the boundary related to the radius $F(\mathbb{E}[q])$, see (2.4), by the black dashed line. It can clearly be seen that this solution differs from the expectation $\mathbb{E}[\Gamma]$ due to the nonlinearity of the problem. This is also indicated by the plot of the related radial functions on the right-hand side of Figure 2. Here, we show the expectation $\mathbb{E}[r](\phi)$ (blue line), the radius $F(\mathbb{E}[q])$ of the solution for the fixed inner boundary $\mathbb{E}[\Sigma]$ (black dashed line), the radius of the inner boundary $\mathbb{E}[q](\phi)$ (green) and the radius of the standard deviation $\sqrt{\mathbb{V}[\Gamma](\phi)}$ (red).

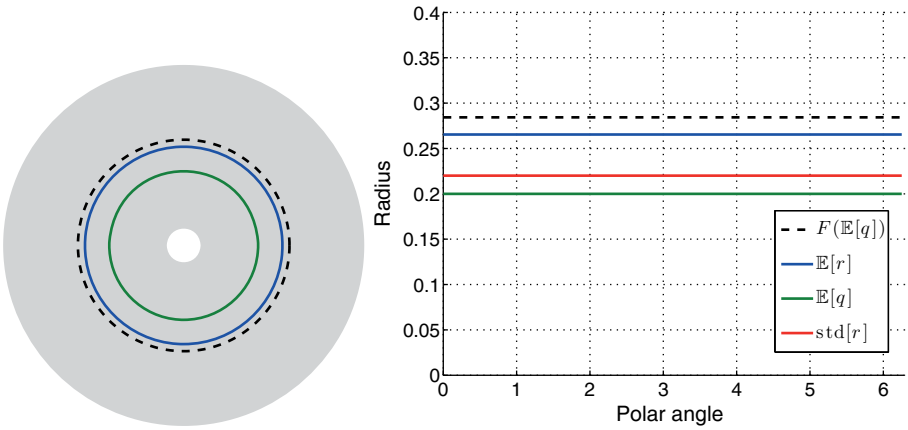

Fig. 2: Expectation of the solution to the free boundary problem (left) and related expectations of the radii (right) for the first example.

In order to make the nonlinearity in the problem better visible, Figure 3, shows the radius $r(\phi, \omega)$ (blue) computed by (2.5) with respect to $q(\phi, \omega) \in [0.005, 0.395]$. Moreover, we have depicted the sensitivity of $r(\phi, \omega)$ with respect to $q(\phi, \omega)$, i.e., the derivative with respect to $q(\phi, \omega)$, in red. As it turns out, we have a strong nonlinearity only for very small values of $q(\phi, \omega)$. For larger values of $q(\phi, \omega)$, the problem exhibits a rather linear behavior. Finally, the black dot in the picture refers to the radius r that is obtained for $\mathbb{E}[q] = 0.2$, i.e., $F(0.2)$, and the blue dot on the secant connecting the extremal values of $r(\phi, \omega)$ (green) refers to $\mathbb{E}[r] = 0.5(F(0.005) + F(0.395))$, cf. (2.4). As they obviously do not coincide, this also confirms the statement (2.6).

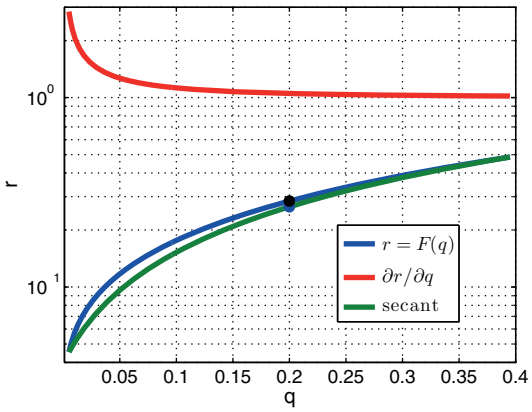

Fig. 3: Dependency and sensitivity of $r(\phi, \omega)$ on $q(\phi, \omega)$.

2.4.2 Second example

For the second example, the same boundary conditions are chosen as in the previous example. Moreover, the radial function of $\Sigma(\omega)$ is defined according to

$$q(\phi, \omega) = 0.25 + 0.05 \sum_{k=1}^{5} \frac{\sqrt{2}}{k} \{ \sin(k\phi) X_{2k-1}(\omega) + \cos(k\phi) X_{2k}(\omega) \} ,$$

where the random variables $\{X_k\}_k$ are independent and distributed with respect to the counting measure μ as before. In the spirit of the previous example, here we have to determine the 1024 realizations of the free boundary related to the 1024 possible realizations of $q(\phi, \omega)$ in order to exactly determine the expectation and the variance of the free boundary. Thus, this example may be considered a more complex version of the previous one.

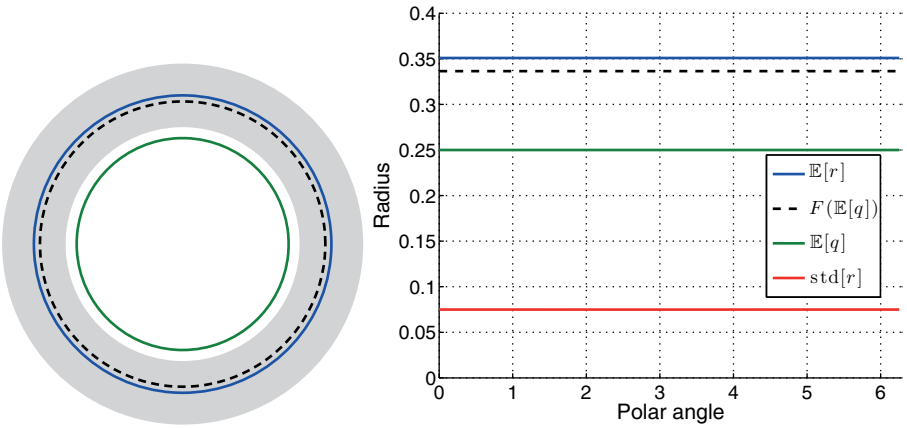

Fig. 4: Expectation of the solution to the free boundary problem (left) and related expectations of the radii (right) for the second example.

Figure 4 visualizes the expectation and the standard deviation of the free boundary and the related radii. On the left hand side, one finds the random domain's statistics and on the right-hand side the associated radial functions. Again, we see that there is a mismatch between the domain's expectation (blue line) and the free boundary which belongs to the expected interior boundary (black dashed line).

2.4.3 Third example

In our third example, we consider the approximation of the expectation and the variance of the solution to (1.3) in the case of a perturbed potato shaped inner domain. For

the data, we prescribe the boundary conditions $u(\omega) = 1$ on $\Sigma(\omega)$ and $\|\nabla u(\omega)\|_2 = 6$ on $\Gamma(\omega)$. The radial function for $\Sigma(\omega)$ is given by

$$q(\phi, \omega) = 0.2 + 0.01 f(\phi) + \sum_{k=1}^{10} \frac{\sqrt{2}}{k} \{ \sin(k\phi) X_{2k-1}(\omega) + \cos(k\phi) X_{2k}(\omega) \} ,$$

where $f(\phi)$ is a trigonometric polynomial with coefficients, cf. (3.5),

$$\begin{aligned} &[a_5, \dots, a_0, b_1, \dots, b_4] \\ &= [0.33, 0.26, 0.51, 0.70, 0.89, 0.48, 0.55, 0.14, 0.15, 0.26] . \end{aligned}$$

The random variables $\{X_k\}_k$ are chosen to be independent and uniformly distributed in $[-1, 1]$. The approximation of the expectation $\mathbb{E}[r](\phi)$ and the variance $\mathbb{V}[r](\phi)$ is performed by the application of a quasi-Monte Carlo quadrature based on 10 000 Halton points, cf. [11]. As already pointed out in Section 2.2.4, the application of the quasi-Monte Carlo quadrature requires mixed smoothness of the integrand. Although this is not proven here, we have strong evidence that the function $r(\phi, \omega)$ exhibits this smoothness. This is also validated by this example.

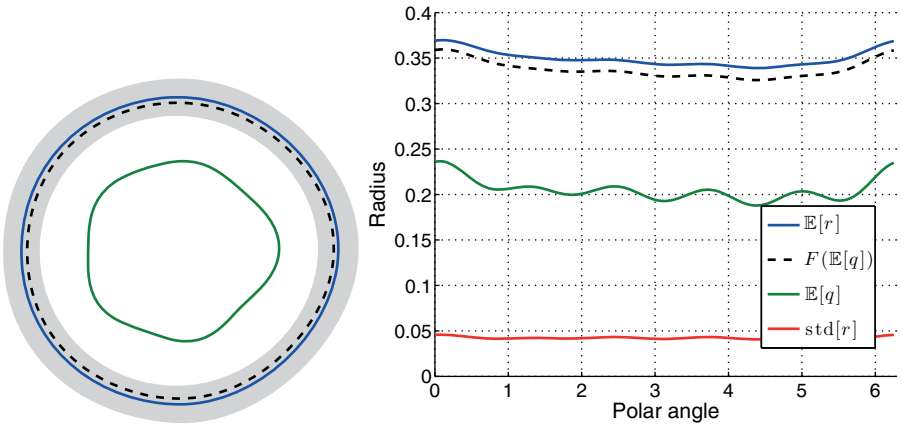

Fig. 5: Expectation of the solution to the free boundary problem (left) and related expectations of the radii (right) for the third example.

On the left-hand side of Figure 5, a visualization of the random domain's statistics is found. The left-hand side of Figure 5 shows the expectation $\mathbb{E}[\Sigma]$ (green) and the expectation $\mathbb{E}[\Gamma]$ (blue). The gray shaded area refers to the standard deviation of Γ. Moreover, the free boundary that corresponds to $\mathbb{E}[\Sigma]$ is indicated by the black dashed line. It differs again clearly from the expectation $\mathbb{E}[\Gamma]$. The right-hand side of Figure 5 shows the related radius functions. Here, the standard deviation is indicated in red.

Finally, in order to justify the application of the quasi-Monte Carlo quadrature based on Halton points, we have also considered the convergence of the Monte Carlo

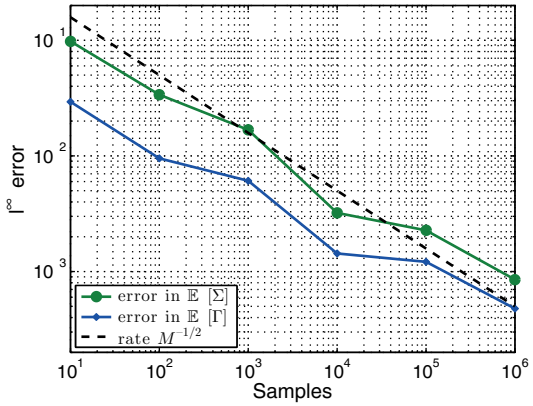

Fig. 6: Convergence of the Monte Carlo quadrature to the approximation based on the quasi-Monte Carlo quadrature.

quadrature toward the approximation of the expectation obtained by the quasi-Monte Carlo quadrature. The related plot is found in Figure 6. The green line refers to the approximation of the expectation of the inner boundary $\mathbb{E}[\Sigma]$, which is a linear problem. The blue line indicates the convergence of the expectation of the outer boundary $\mathbb{E}[\Gamma]$, which is a nonlinear problem. We have measured here the relative error in the ℓ^∞-norm of the boundaries evaluated in the collocation points. The theoretical rate of convergence, given by $M^{-1/2}$, where M denotes the number of Monte Carlo samples, is visualized by the black dashed line. As it turns out, we obtain in both cases convergence of the Monte Carlo quadrature toward the solution obtained by the quasi-Monte Carlo quadrature. This validates the approximation obtained by the quasi-Monte Carlo quadrature, which will also be used as the stochastic quadrature method in the following example.

2.4.4 Fourth example

Finally, we consider an example where the inner boundary $\Sigma(\omega)$ is given by four circles of radius 0.05 with randomly varying midpoints

$$[0.1(-1)^i + 0.04X_{2(2i+j)}(\omega), 0.1(-1)^j + 0.04X_{2(2i+j)+1}(\omega)]^\intercal \quad \text{for } i, j = 0, 1\,.$$

Here, the random variables $X_1, \ldots, X_8$ are independent and uniformly distributed on $[-1, 1]$. The radii and midpoints of the circles are chosen such that they cannot overlap. In order to illustrate the situation under consideration, we have depicted six different realizations of $\Sigma(\omega)$ and of the related free boundaries $\Gamma(\omega)$ in Figure 7.

For this example, the boundary conditions are chosen as $u(\omega) = 1$ on $\Sigma(\omega)$ and $\|\nabla u(\omega)\|_2 = 8$ on $\Gamma(\omega)$. The visualization of the computed expectation and the standard deviation of the free boundary as well as the related radii are presented in Figure 8. Even though the interior boundaries vary a lot, the difference between the free boundary related to $\mathbb{E}[\Sigma]$ and $\mathbb{E}[\Gamma]$ is relatively small.

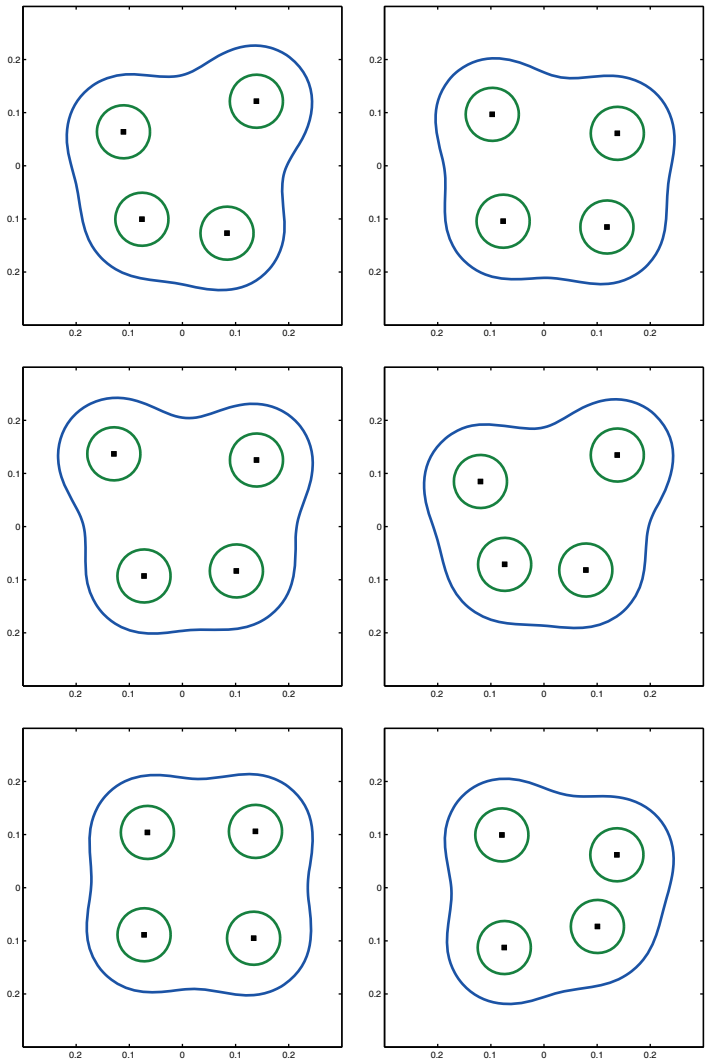

Fig. 7: Different realizations of the random boundary $\Sigma(\omega)$ and corresponding free boundary $\Gamma(\omega)$ for the fourth example.

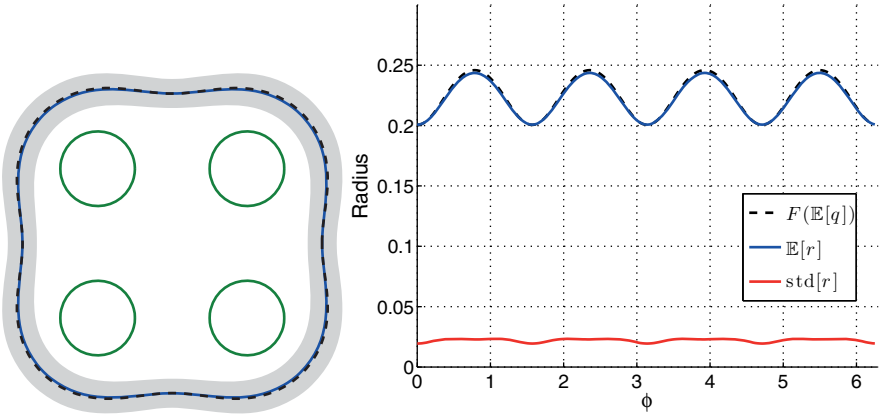

Fig. 8: Expectation of the solution to the free boundary problem (left) and related expectations of the radii (right) for the fourth example.

2.5 Conclusion

In the present chapter, Bernoulli's exterior free boundary problem has been considered in the case of an interior boundary which is random. Such uncertainties may arise from tolerances in fabrication processes or from measurement errors. We modeled this problem mathematically and showed its well posedness. Expectation and variance of the resulting random domain have been introduced and numerically computed. Establishing regularity results with respect to the random parameter will be subject of future work in order to rigorously prove the convergence of the present quasi-Monte Carlo method and even more sophisticated quadrature methods.

Bibliography

[1] A. Acker, On the geometric form of Bernoulli configurations, *Mathematical Methods in the Applied Sciences*, 10(1):1–14, 1988.

[2] A. Acker and R. Meyer, A free boundary problem for the p-laplacian: uniqueness, convexity, and successive approximation of solutions, *Electronic Journal of Differential Equations*, 8:1–20, 1995.

[3] H. W. Alt and L. A. Caffarelli, Existence and regularity for a minimum problem with free boundary, *Journal für die reine und angewandte Mathematik*, 325:105–144, 1981.

[4] A. Beurling, On free boundary problems for the Laplace equation, *Seminars on Analytic functions, Institute for Advanced Study, Princeton, NJ*, 1:248–263, 1957.

[5] R. Caflisch, Monte Carlo and quasi-Monte Carlo methods, *Acta Numerica*, 7:1–49, 1998.

[6] M. Crouzeix, Variational approach of a magnetic shaping problem, *European Journal of Mechanics B-Fluids*, 10:527–536, 1991.

[7] J. Descloux, Stability of the solutions of the bidimensional magnetic shaping problem in absence of surface tension, *European Journal of Mechanics B-Fluids*, 10:513–526, 1991.

[8] J. Dölz, H. Harbrecht and M. Peters, $\mathcal{H}$-matrix accelerated second moment analysis for potentials with rough correlation, *Journal of Scientific Computing*, 65:387–410, 2015.
[9] M. Flucher and M. Rumpf, Bernoulli's free-boundary problem, qualitative theory and numerical approximation, *Journal für die Reine und angewandte Mathematik*, 486:165–204, 1997.
[10] A. Friedman, Free boundary problem in fluid dynamics, *Astérisque*, 118:55–67, 1984.
[11] J. H. Halton, On the efficiency of certain quasi-random sequences of points in evaluating multi-dimensional integrals, *Numerische Mathematik*, 2(1):84–90, 1960.
[12] H. Harbrecht and G. Mitrou, Improved trial methods for a class of generalized Bernoulli problems, *Journal of Mathematical Analysis and Applications*, 420(1):177–194, 2014.
[13] H. Harbrecht, M. Peters and M. Siebenmorgen, Efficient approximation of random fields for numerical applications, *Numerical Linear Algebra with Applications*, 22:596–617, 2015.
[14] E. Hille and R. S. Phillips, *Functional analysis and semi-groups*, volume 31, American Mathematical Society, Providence, 1957.
[15] R. Kress, *Linear integral equations*, Vol. 82 of Applied Mathematical Sciences. Springer, New York, 2nd edition, 1999.
[16] M. Loève, *Probability theory. I+II*, Number 45 in Graduate Texts in Mathematics. Springer, New York, 4th edition, 1977.
[17] D. E. Tepper, On a free boundary problem, the starlike case, *SIAM Journal on Mathematical Analysis*, 6(3):503–505, 1975.
[18] T. Tiihonen and J. Järvinen, On fixed point (trial) methods for free boundary problems, In S. N. Antontsev, A. M. Khludnev and K.-H. Hoffmann, editors, *Free Boundary Problems in Continuum Mechanics*, volume 106 of *International Series of Numerical Mathematics*, pp. 339–350. Birkäuser, Basel, 1992.